Power System Technology
ISSN:1000-3673

Received: 16-04-2025 *Revised: 05-05-2025* *Accepted: 22-06-2025*

Parametric Analysis of Wind Load Effects on Cable-Stayed Bridges Across Diverse Wind Angles and Climatic Regions Using SAP2000

Rina Kumari[1], Prof S. S Mishra[2]

Research scholar[1], Department of Civil Engineering, N.I.T Patna

Professor[2] Department of Civil Engineering, N.I.T Patna

ABSTRACT

This research article provides a complete parametric analysis of the effects of wind loads on cable-stayed bridges, utilizing the Quincy Bayview Bridge as a case study. The study applies sophisticated finite element analysis using SAP2000 to model the bridge's structural response under varying wind conditions. A realistic model of the bridge is created, depicting its precise geometry, material qualities, and dynamic interactions between components such as double-plane stay cables and concrete pylons. The analysis looks at the bridge's performance at various wind angles (0°, 30°, 45°, 60°, and 90°) and speeds, as prescribed by IS 875 (Part 3), in different climatic zones including Pune, Mumbai, and Delhi. Displacement, base reaction, and bending moments are key metrics that are used to assess the structural integrity and resilience of the bridge. The findings provide important insights into the bridge's dynamic behavior, illustrating how differences in wind angles and speeds affect lateral and vertical motions, internal stresses, and pressures applied on supports. The results highlight the susceptibility of cable-stayed bridges to aerodynamic forces, underlining the need of extensive testing throughout the design phase to reduce the dangers associated with aerodynamic instability. This research intends to contribute to the creation of more robust and efficient bridge designs by identifying crucial performance indicators and possible weak areas, thereby improving the safety and durability of cable-stayed bridges under varying environmental circumstances. The study closes with suggestions for future design methods and research initiatives to improve the structural performance of these critical infrastructure components.

Keywords: Cable-Stayed Bridges, SAP 2000, wind load, angle of attack, Seismic Performance, Finite Element Analysis, etc.

1. INTRODUCTION

Cable-stayed bridges are one of the most aesthetically appealing and popular bridges worldwide due to their advantages i.e., lightweight, relatively small cross-sections, and high structural efficiency. Meanwhile, the race for achieving a longer span cable-stayed bridge is entering a new era with the Russky Bridge (with a main span of 1104 m) holding the current world record. On the other hand, cable stayed bridges are characterized by low structural damping, complex dynamic behavior and longer natural time periods [1]Their relatively small section and lighter weight make them susceptible to oscillations under dynamic loadings such as wind, earthquake, pedestrian and traffic loads. Moreover, as the span length of cable-stayed

Power System Technology
ISSN:1000-3673
Received: 16-04-2025 Revised: 05-05-2025 Accepted: 22-06-2025

bridges increases, the flexibility of the structure and the length of stay cables also increase, which may result in aerodynamic stability issues.

1.1 Necessity of Wind Analysis for Cable-Stayed Bridges:

Many dynamic stresses, such as those caused by traffic, wind, pedestrians, and seismic activity, may affect cable-stayed bridges[2]. Furthermore, the stay cables have very little inherent damping and are quite flexible.
These bridges' geometric and structural characteristics are also quite intricate.
In addition to this, it is still unclear what the precise nature of excitation is and the mechanism behind part of the vibration phenomena is the non-linearity of the geometry and material is the most significant characteristic of this kind of construction[3].

1.2 Need for Wind Analysis

Any building is affected by wind in three distinct ways. They are aerodynamic, dynamic, and static. The kind of structure determines how it will react to a load[4]. When examining how a structure reacts to wind stress, it is important to consider both the static and aerodynamic impacts. Wind affects structural elements that are thin and flexible both along and across the wind's path of action.

Bridges supported by cables are very flexible and have very little inherent dampening. They are often exposed to a range of dynamic stresses, including wind, earthquake, and vehicle loads[5]. Complex geometrical and structural characteristics characterize cable-stayed bridges. The nonlinearity of the material and design of this bridge is one of its most remarkable aspects. In addition to them, it is still unclear exactly what the process and exact kind of stimulation are that lead to the production of vibrations[6].

1.2.1 Types of Wind Induced Vibrations

The cables of a cable-stayed bridge are constructed by wrapping wires or strands composed of fiber-reinforced polymers (FRP) or steel. Their low damping qualities, suppleness, and light weight make them well-liked. When exposed to wind, they may oscillate violently and get readily aroused. A variety of processes and conditions may cause vibrations in cables. The vibrations of the pylon towers and bridge deck are connected with those of the cable[7].

Therefore, the primary cause of vibration on the other structural elements of the bridge is vibration on the cables. The various vibrations caused by wind are as follows:

1 Aerodynamic Galloping

Galloping due to wind effect means the wave like motion of elongated bodies which are not aerodynamic in shape (bluff bodies). In the case of a cable-stayed bridge the bluff body is usually the bridge deck. So aerodynamic galloping is the oscillation of bridge deck when acted upon by wind.It is a low frequency situation and therefore does not create an adverse effect usually.

Power System Technology
ISSN:1000-3673
Received: 16-04-2025 Revised: 05-05-2025 Accepted: 22-06-2025

2 Wake Galloping

Wake galloping is the vibration of the bridge deck induced due to the wake effect formed between cables. When wind is acted on two cables which are spaced close to each other, a force or wake effect is developed between the cables. Under the action of this force the cables tend to rotate in opposite directions which induces torsional oscillations. This vibration is transmitted to the bridge deck which in turn causes galloping effect on the deck.

3 Buffeting

Buffeting is the sudden instability occurred due to shock wave oscillations or air flow separation created when two objects strike each other. Sudden impact of a seismic load or dynamic load leads cables to strike one another. This sudden shock induces vibration on the whole structure. Buffeting is a high frequency phenomena.

4 Vortex Shedding

When air flows past a slender and tall body at certain velocities, an oscillation is experienced. This oscillating force is called vortex shedding. In the case of a cable-stayed bridge pylons are prone to experience this effect. When wind flows past the pylon, low pressure vortices are formed on the downstream side of it. This vortex force will be likely to move the pylon from side to side. If the vortex shedding frequency becomes equal to resonance frequency of the structure, the whole structure will vibrate with harmonic oscillations. Vortex shedding is a higher frequency phenomena and it depends mainly on the size and shape of the pylon.

5 Fluttering

Fluttering is an unstable vibratory motion of the structure due to the coupling between elastic deformation of the structure and the aerodynamic force acted on it. Fluttering occurs due to the combined effect of bending and torsion. Long span bridges like suspension bridge and cable-stayed bridges are more prone to fluttering because of their large d/t value, d being the depth of structure parallel to wind and t being the least lateral dimension. Fluttering is a major vibratory motion and has even lead the collapse of Tacoma Narrows cable-stayed bridge in 1940.

6 Resonant buffeting

Resonant buffeting occurs in bridges with 2 parallel planes of cables. This phenomena happens mainly due to the wake effect formation between the cables. Wind striking the upwind and downwind portions of the cable with a time delay induces the whole cables to move laterally.

Power System Technology
ISSN:1000-3673
Received: 16-04-2025 Revised: 05-05-2025 Accepted: 22-06-2025

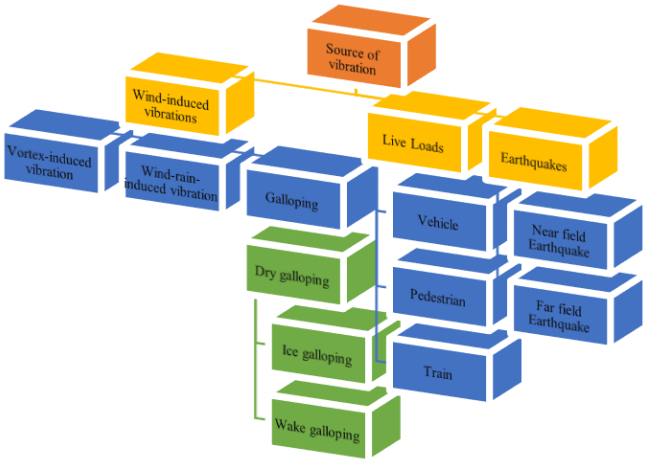

Fig. 1: Different types of dynamic loads in the cable stayed bridges[8]

As shown in above figure, stay cables are generally subjected to direct vibration due to the wind acting along the cable and indirect vibration through cable anchorages at the deck and towers due to wind, traffic, and earthquake loads.

The optimization of cable-stayed bridges is a difficult issue for structural engineers. Although the first studies on this issue were published over 40 years ago, it is now a popular study area, with more than half of the studies published in the previous decade. Traditionally, optimization methods were used to optimize cable forces and design, with the goal of minimizing costs. 80% of past research on the optimization of cable-stayed bridges was focused on these two problems. However, in the last decade, there has been a growing interest in applying optimization algorithms to a variety of applications, including the design of hybrid fiber reinforced polymeric deck and cables, monitoring and assessment of existing bridges, and the design of passive and active control devices to improve seismic performance. Cable-stayed bridges are made up of three primary structural elements: decks, towers, and cable-stays. They have many inclined cable stays that help to sustain the deck throughout its length. This enables for the building of large-span bridges with shallow decks. The deck functions as a continuous beam elastically supported by inclined stays, which offer vertical support as well as natural prestressing in the deck. The cable-stays convey the deck's vertical stresses to the towers. The towers' compression transfers the weight to the foundations. These bridges are extremely redundant, with their behavior determined by the stiffness of the load-supporting parts (deck, towers, and cable stays) as well as the distribution of cable forces. They provide an effective structural solution for medium-to-long spans and are extensively utilized across the globe. The slenderness of the deck and the design of the cable suspension system give these constructions obvious visual appeal. The graphic below depicts the weight transfer method in a symmetrical cable-stayed bridge. Several publications provide detailed explanations of the major characteristics and structural behavior of cable-stayed bridges [9], [10].

Power System Technology
ISSN:1000-3673
Received: 16-04-2025 Revised: 05-05-2025 Accepted: 22-06-2025

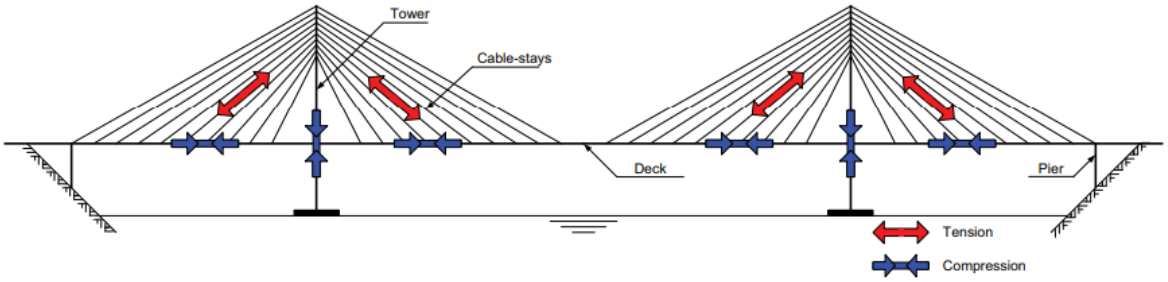

Fig. 2: Scheme of load transfer in a cable-stayed bridge [11]

The design of cable-stayed bridges is a difficult process that entails solving a number of complex problems, including the defining of the structural system, the determination of member cross-sections, the calculation of cable forces distribution, building phases, and geometric nonlinear effects. For concrete bridges, time-dependent effects are critical and must be addressed. Optimization techniques are especially well suited to solving design problems in big and complex structures such as cable-stayed bridges. They offer an effective technique to handle large amounts of information with the goal of lowering material prices and creating affordable and structurally efficient solutions. Furthermore, because of their decision-making skills, these techniques are well-suited to solving a variety of problems in these complex structures [11].

The aim of this study is to conduct a parametric analysis of wind load effects on cable-stayed bridges across diverse wind angles and climatic regions using SAP2000. The study seeks to comprehensively evaluate the dynamic response of a cable-stayed bridge model under varying wind conditions, considering the interaction between structural components and the effects of different wind angles and regional wind speeds. By employing advanced simulation techniques, the research aims to identify critical performance indicators and contribute to the development of more resilient and efficient bridge designs in the context of varying environmental conditions.

2. LITERATURE REVIEW

Feder [11] presented an optimality criterion method for calculating cable prestressing forces in steel bridges. The optimality criteria included cable strains and bending moments in the main girder and tower base. The influence coefficients of the cable forces were employed, and the issue was formulated as a system of linear equations solved using the least squares method. To optimize cable forces in concrete bridges with prestressed decks while taking into account the concrete creep effect, Furukawa et al[12]. also applied the minimization of a strain energy criteria. The tendon forces in the main girder were described as linear functions of cable forces.

Qin [13] investigated the construction phases of segmental cantilever construction and addressed the optimal cable-stretching planning using a linear programming (LP) problem. In concrete cable-stayed bridges, Kasuga et al[14]. studied cable force modifications, including the cable creep effect. An effect matrix of the cable forces was employed, and the adjustment

Power System Technology
ISSN:1000-3673
Received: 16-04-2025 Revised: 05-05-2025 Accepted: 22-06-2025

forces were determined using a nonlinear programming (NLP) problem and work minimization owing to these forces. Wang et al.[15] studied four techniques to optimize cable forces in order to reduce deformations and stresses caused by the bridge's dead load. The authors investigated the following: minimization of the sum of the squares of the vertical displacements of the cable anchor points at the deck (MMSVD); minimization of the maximum moment along the bridge deck (MMM); continuous beam method (CBM); and simply supported beam method (SBM). The latter was chosen as the optimum method after comparing the estimated bending and vertical displacements of the bridge deck. Janjic et al.[16] introduced the unit force method (UFM) to calculate cable forces in order to achieve the required deck bending moment distribution for the whole bridge under dead load. The method incorporates the construction sequence, geometrical nonlinearities, and time-dependent phenomena such as concrete creep and shrinkage, as well as prestressing tendon relaxation. The optimization of cable forces for asymmetric steel bridges was addressed by Sung et al.[17] and Lee et al.[18].

Sung et al.[19] employed a cable force effect matrix and the minimization of total strain energy defined as a quadratic function of post-tensioning cable forces. To obtain the appropriate deck bending moment distribution for the structure's final stage under dead load and cable prestressing forces, Lee et al.[18] applied a two-step methodology based on the unit load method. Sun et al.[20] utilized the trust region algorithm to calculate the appropriate cable forces for the bridge's deck and towers that minimize the bending strain energy under permanent loads. Baldomir and Hernández [21], Baldomir et al. [22], and Hernandez et al. [23] found the cable areas for a long span steel bridge by minimizing the cable volume using a gradient-based sequential quadratic programming (SQP) algorithm using finite difference sensitivity. Zhang and Bai [24] calculated the cable forces for a single-pylon, double-plane concrete bridge. The least bending strain energy was utilized to represent the objective function as a quadratic form of the cable prestressing forces. The ANSYS parametric design language (APDL) was employed to resolve the optimization problem. Yu et al.[25] utilized the Midas/Civil software's unknown load factor method (ULF) to optimize an asymmetrical bridge's cable forces. This method makes use of the impact matrix notion, and the displacements, responses, and internal forces of members may all be considered constraints. By minimizing the square root of sum of squares (SRSS) of the deck and tower nodal points' deflections, Hassan et al. [26] calculated the cable forces in steel - concrete composite bridges. Hassan [26] utilized the same algorithm to obtain cable areas via minimization of the steel weight of the cables. In both papers, B-spline interpolation curves were used to characterize the distribution of cable forces and to effectively manage the large number of variables that occur as a result of the many cables. Sun et al. [27] suggested an optimization method for calculating cable forces based on construction phases, with the goal of achieving the desired final state upon bridge completion. The forward analysis approach was utilized to model the construction process. The optimization was designed as a quadratic programming problem to minimize the difference between the bridge's determined and ideal final states.

Zhang et al. [28] presented a two-stage technique to obtaining the best cable tensions for hybrid cable-stayed suspension bridges under dead load. The finite element method (FEM) with geometrical nonlinearities and a constraint relaxation quadratic programming method were used. Lonetti and Pascuzzo [29] devised a method for obtaining the best post-tensioning cable

Power System Technology
ISSN:1000-3673
Received: 16-04-2025 Revised: 05-05-2025 Accepted: 22-06-2025

forces and cable cross-sections for self-anchored cable-stayed suspension bridges. The FEM was utilized to do structural analysis with geometrical nonlinearities, dead and live loads. Constraints on ultimate and serviceability limit states, maximum allowed stresses, and bridge deflections were evaluated. A sparse nonlinear optimizer (SNOPT) was utilized to tackle a restricted nonlinear programming (NLP) problem. Martins et al.[30] determined cable forces while taking into account construction phases, time-dependent effects of concrete, and geometrical nonlinearities [28]) and [30]. The solution was discovered by minimizing a constraint aggregation (displacements and stresses) convex scalar function produced using an entropy-based method. In terms of long-span optimization, Asgari et al. [31] proposed a multiconstraint technique based on the application of an inverse problem via the unit load method. By minimizing the weighted total bending energy of the girder and the tower, Song et al. [32] determined the cable forces, load, and counterweight range in long-span bridges.

Sun and Xiao [32] proposed a method for the optimization of the dead load state in earth-anchored cable-stayed bridges. The method is based on the rigidly supported continuous beam method as well as the feasible zone method. The ANSYS APDL language was utilized for the optimization of self-anchored cable forces via the minimization of cable strain energy. The earth-anchored cable forces were optimized using the feasible zone of pylon bending moments. Using the cantilever erection method, Sung et al.[33] addressed optimal construction planning. The cable forces were calculated using the minimization of the difference between completion displacements and pre-planned construction objectives. During each construction step, constraints on the cables' axial forces were considered. To increase the ability to escape local minimums, particle swarm optimization (PSO) and simulated annealing (SA) were merged into a traditional genetic algorithm's (GA) mutation process. Carpentieri et al. [34] created an algorithm for designing the cables' pre-tensioning sequence optimally. The cables' pre-tensioning forces, which create a "optimal" bending moment distribution throughout the deck, were determined by solving a linear problem. Fabbrocino et al. [34] computed the cable prestressing forces in bridges with steel-concrete composite decks to obtain the necessary bending moment distribution over the longitudinal beams. An influence matrix of cable forces was used, and the target cable moment distribution was developed with the goal of making the most of the materials that make up the bridge.

Ha et al. [35] used a nonlinear inelastic analysis to develop a three-stage algorithm for optimizing the initial cable tensions and overall weight of the cables. We present a micro-genetic algorithm (μGA)-based method using a unit load matrix to decrease computing effort. Through the minimization of the SRSS of the deck vertical and pylon horizontal deflections, the initial cable tensions were obtained. The cable areas were calculated using the minimization of the overall weight of the cables, taking into account the tensions beneath the bridge's dead and active cables as well as the previously computed starting cable tension. The stresses on the bridge's member strain and deck vertical and deck horizontal deflections were considered. Baldomir et al. [36] reduced the cable volume of the Forth Replacement Crossing Bridge when it comes to multi-span bridges. To achieve the necessary geometry under self-weight, two design factors per stay were considered: the cross sectional area and the prestressing force. The optimization problem was solved using the commercial program Altair Optistruct v11 (2013). Cid et al. [37] determined the cable anchor locations, areas, and forces in a multi-span bridge

Power System Technology
ISSN:1000-3673
Received: 16-04-2025 Revised: 05-05-2025 Accepted: 22-06-2025

with steel towers and cable deck, taking into account the geometrical nonlinearities. The cable steel volume minimization was carried out using a gradient-based SQP algorithm, and the sensitivities were calculated using finite differences. Arellano et al. [38] also studied multi-span bridges to calculate cable overlap lengths in bridges with crisscross cables. As objective functions, the cable system's minimal cost, the minimum maximum displacement of the pylon head, and the maximum alternative live load on the bridge were considered. The multi-objective problem was addressed with the non-dominated sorting genetic algorithm II (NSGA II).

Performance-based design is an approach in which structural criteria are articulated in terms of meeting a performance objective. This is in contrast to the traditional method, which defines structural requirements as limitations on member forces caused by a certain level of applied shear force. A performance objective outlines the intended seismic performance of a structure. The highest permissible damage state (performance level) for a given design hazard is used to define seismic performance. A performance objective that takes into account damage states at various levels of ground motion is referred to as a dual or multiple level performance objective [39].
Non-linear static analysis, also known as pushover analysis, is a powerful method for measuring inelastic strength and deformation demands in structures, as well as uncovering design flaws [39]. Its primary benefit is that it allows the design engineer to determine significant seismic response quantities and utilize engineering judgment to appropriately modify the force and deformation demands and capabilities that regulate the seismic response near failure. The pushover analysis generates a force-displacement curve known as the pushover curve. It is a plot of base shear (total lateral load) vs lateral displacement at a specific position on the roof level, including all stages of lateral load / load increments. It should be highlighted that the pushover analysis is just approximate and does not take into consideration dynamic features such as hysteresis, increased mode involvement, and so on. It is known to provide excellent outcomes for normal structures (with no torsional irregularity). The pushover curve may be transformed to an acceleration versus displacement response spectrum, indicating the structure's "seismic capacity." Including "seismic demand" in the same plot may help determine whether capacity matches demand. A performance point is defined as the moment at which seismic capacity and demand coincide [40].

3. METHODOLOGY

The study's methodology involves a systematic approach to analyze the wind load effects on a cable-stayed bridge using SAP2000. The process begins with the development of an accurate and detailed model of the bridge in ETABS, capturing the intricate geometry and material properties of the Quincy Bayview Bridge, including its double-plane stay cables and concrete pylons. The modeling process integrates dynamic interactions between the bridge components, ensuring a realistic simulation environment. Various wind angles (0°, 30°, 45°, 60°, 90°) and wind speeds corresponding to different climatic regions (Pune, Mumbai, and Delhi) are applied to the model based on data from IS 875 (Part 3). The simulation results are then analyzed to evaluate the bridge's performance under these different scenarios, focusing on the structure's dynamic response to wind loads, potential for progressive collapse, and overall integrity. The

Power System Technology
ISSN:1000-3673
Received: 16-04-2025 Revised: 05-05-2025 Accepted: 22-06-2025

findings are subsequently discussed, leading to the development of conclusions and recommendations aimed at enhancing the structural resilience of cable-stayed bridges in diverse environmental conditions.

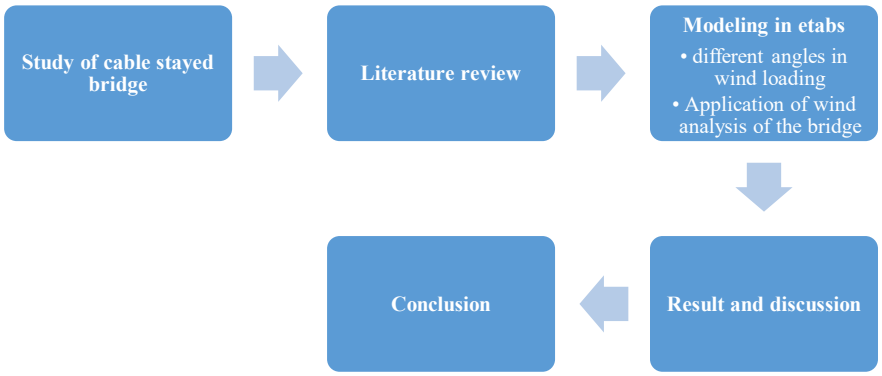

Fig. 3: Methodology of Work

3.1 Bridge details

The geometry of the selected bridge for this study is similar to the Quincy Bayview Bridge, located in Illinois, USA. The length of the main span (M) is 285.6 m, with two side spans (S) of 128.1 m. Therefore, the total length of the bridge (L) is 541.8 m. The deck superstructure is supported by double planes of stay cables in a semi-harp type arrangement, where forty cables are anchored into each transverse H frame-shaped pylon. As such, eighty stay cables support the entire bridge deck, with forty supporting the main span and twenty cables supporting each side span. The bridge has two lanes of traffic with a width of 12.2 m measured between centers of the cables. The typical cross-section of the bridge deck consists of a precast concrete deck having a thickness of 0.23 m and a width of 14.20 m. Two steel main girders are located at the outer edge of the deck. These girders are interconnected by a set of equally spaced floor steel beams. The distance between each pair of floor steel beams is 9.0 meters The pylons consist of two concrete legs, interconnected with a pair of struts. The upper strut cross beam connects the upper legs and the lower strut cross beam supports the deck. The lower legs of the pylon are connected by a 1.22 m thick wall, which is placed as a web between the two legs[41].

3.2 Material Properties:

The materials employed in the construction of the cable-stayed bridge encompass concrete and steel for specific components. The reinforced pylon and box girder utilize concrete with the following properties. For the cables, steel is employed with distinct properties. These material specifications are crucial considerations in ensuring the structural integrity and performance of the cable-stayed bridge, with each component designed to meet the required standards for strength, elasticity, and density.

Power System Technology
ISSN:1000-3673
Received: 16-04-2025 Revised: 05-05-2025 Accepted: 22-06-2025

Table 1: Material properties of the bridge

Steel	Modulus of elasticity, (Es)	= 200 GPa
	Unit weight, (γs	= 77 kN/m3
	Poisson's ratio, (vs)	= 350 MPa
	Yield strength, (Fy)	= 0.30
Concrete	Modulus of elasticity, (Ec)	= 24.87 GPa
	Unit weight, (γc)	= 24.0 kN/m3
	Poisson's ratio, (vc)	= 0.20
	Compressive strength, (fc')	= 30 MPa
Cables	Modulus of elasticity, (Esc)	= 205 GPa
	Unit weight, (γscable)	= 82.40 kN/m3
	Ultimate tensile strength, (TcCable)	= 1.6 GPa

- **Modeling details**

The modeling details consist of three cases, each representing a different region with varying wind speeds and angles. In Case 1, the region is Pune with a wind speed of 39 m/s. The wind angles considered for this case are 0 degrees, 30 degrees, 45 degrees, 60 degrees, and 90 degrees. For Case 2, the region is Mumbai with a wind speed of 44 m/s, and the same wind angles of 0 degrees, 30 degrees, 45 degrees, 60 degrees, and 90 degrees are used for analysis. Finally, in Case 3, the region is Delhi with a wind speed of 47 m/s, where the wind angles evaluated are also 0 degrees, 30 degrees, 45 degrees, 60 degrees, and 90 degrees. Each case studies the impact of varying wind angles on the structure based on the specific wind speeds of the respective regions.

Note: Wind speed taken from IS: 875(Part3): Wind Loads on Buildings and Structures - Proposed Draft & Commentary

Source: [41]

The basic wind speed for any site shall be obtained and shall be modified to include the following effects to get design wind speed,

Power System Technology
ISSN:1000-3673
Received: 16-04-2025 Revised: 05-05-2025 Accepted: 22-06-2025

Vz at any height, Z for the chosen structure:

(a) Risk level, (b) Terrain roughness and height of structure, (c) Local topography, and (d) Importance factor for the cyclonic region.

It can be mathematically expressed as follows:

Vz = Vb x k1 x k 2 x k3 x k4,

where Vz = design wind speed at any height

z in m/s, k1 = probability factor (risk coefficient) (see 5.3.1 from IS 875 part 3),

k2 = terrain roughness and height factor (see 5.3.2 from IS 875 part 3),

k3 = topography factor (see 5.3.3 from IS 875 part 3), and

k4 = importance factor for the cyclonic region (see 5.3.4 from IS 875 part 3).

For the given bridge, the width of the bridge deck is 24.4 meters, the length is 14.2 meters, and the height for wind exposure calculations is 69.8 meters. The basic wind speeds considered are 39 m/s, 44 m/s, and 47 m/s, with Terrain Category 1. The importance factor k1 is taken as 1.15, the risk coefficient is 1.0, the topography factor k3 is 1.0, and the windward coefficient Cp is 0.8, while the leeward coefficient is 0.5.

To calculate the wind loads acting on a structure, we first determine the design wind speed at a height of 0 meters. The design wind speed is adjusted for height, terrain, importance, and topography. Given the basic wind speed of 47 meters per second, and with coefficients for height and terrain, we calculate the design wind speed to be approximately 2319.45 meters per second. Next, we calculate the wind pressure using the formula that incorporates the square of the design wind speed. This results in a wind pressure of approximately 1391.67 Newtons per square meter, equivalent to 1.391 KN.

Moving on to the wind load on the structure, we have specified dimensions: a width of 24.4 meters, a height of 69.8 meters, and a length of 14.2 meters. We start by calculating the effective area for various angles of wind incidence. At zero degrees, the effective area is about 1703.12 square meters. At thirty degrees, the effective area increases to approximately 1970.48 square meters. At forty-five degrees, it is around 1904.86 square meters. At sixty degrees, the area is about 1709.90 square meters. Finally, at ninety degrees, the effective area is approximately 991.16 square meters.

Using the calculated wind pressure and a windward coefficient of 0.8, we can calculate the wind load for each angle. At zero degrees, the wind load is approximately 2275.37 KN. At thirty degrees, the load increases to around 2632.56 KN. At forty-five degrees, the wind load is about 2544.89 KN. At sixty degrees, it is approximately 2284.43 KN, and at ninety degrees, the wind load is around 1324.19 KN.

Power System Technology
ISSN:1000-3673
Received: 16-04-2025 Revised: 05-05-2025 Accepted: 22-06-2025

Next, we consider the leeward side of the structure, using a leeward coefficient of 0.5. For the leeward side at zero degrees, the wind load is about 1422.11 KN. At thirty degrees, the load is approximately 1645.35 KN. At forty-five degrees, it is around 1590.55 KN. At sixty degrees, the leeward load is about 1427.77 KN, and at ninety degrees, it is approximately 827.62 KN.

Finally, we combine the windward and leeward forces to calculate the total wind load on the bridge deck for each angle. At zero degrees, the total wind load is approximately 853.26 KN. At thirty degrees, the total load is around 987.21 KN. At forty-five degrees, the total wind load is about 954.33 KN. At sixty degrees, it is approximately 856.66 KN, and at ninety degrees, the total wind load is around 496.57 KN. These calculations provide essential insights into the total wind load acting on the structure, ensuring its structural integrity against wind forces.

3.3 Summary of calculations:

Pune region:

Table 2: Pune region

Height	K1	K2	K3	V_b	V_z	P_z	P_z in KN
0	1	1.05	1	39	1597.05	958.23	0.95823
15	1	1.09	1	39	1657.89	994.734	0.994734
20	1	1.12	1	39	1703.52	1022.112	1.022112
30	1	1.15	1	39	1749.15	1049.49	1.04949
50	1	1.2	1	39	1825.2	1095.12	1.09512
100	1	1.26	1	39	1916.46	1149.876	1.149876

wind angle	Area at different angles	$F_{windward}$	$F_{leeward}$	F_{total}
0	1703.12	1305.58454	815.990339	489.5942
30	1970.48192	1568.08429	980.052681	588.0316
45	1904.85596	1557.58091	973.488067	584.0928
60	1709.90456	1435.62219	897.263868	538.3583
90	991.16	868.351311	542.71957	325.6317

Power System Technology
ISSN:1000-3673
Received: 16-04-2025 Revised: 05-05-2025 Accepted: 22-06-2025

Mumbai region:

Table 3: Mumbai region

Height	K1	K2	K3	V_b	V_z	P_z	P_z in KN
0	1	1.05	1	44	2032.8	1219.68	1.21968
15	1	1.09	1	44	2110.24	1266.144	1.266144
20	1	1.12	1	44	2168.32	1300.992	1.300992
30	1	1.15	1	44	2226.4	1335.84	1.33584
50	1	1.2	1	44	2323.2	1393.92	1.39392
100	1	1.26	1	44	2439.36	1463.616	1.463616

wind angle	Area at different angles	$F_{windward}$	$F_{leeward}$	F_{total}
0	1703.12	1661.80912	1038.6307	623.1784
30	1970.48192	1995.93109	1247.45693	748.4742
45	1904.85596	1982.56189	1239.10118	743.4607
60	1709.90456	1827.32713	1142.07945	685.2477
90	991.16	1105.2782	690.798874	414.4793

Delhi region:

Table 4: Delhi region

Height	K1	K2	K3	V_b	V_z	P_z	P_z in KN
0	1	1.05	1	47	2319.45	1391.67	1.39167
15	1	1.09	1	47	2407.81	1444.686	1.444686
20	1	1.12	1	47	2474.08	1484.448	1.484448
30	1	1.15	1	47	2540.35	1524.21	1.52421
50	1	1.2	1	47	2650.8	1590.48	1.59048

Power System Technology
ISSN:1000-3673
Received: 16-04-2025 Revised: 05-05-2025 Accepted: 22-06-2025

100	1	1.26	1	47	2783.34	1670.004	1.670004

wind angle	Area at different angles	$F_{windward}$	$F_{leeward}$	F_{total}
0	1703.12	2275.36832	1422.1052	853.2631
30	1970.48192	2632.56385	1645.3524	987.2114
45	1904.85596	2544.88756	1590.55473	954.3328
60	1709.90456	2284.43249	1427.77031	856.6622
90	991.16	1324.18976	827.6186	496.5712

3.4 Modeling images:

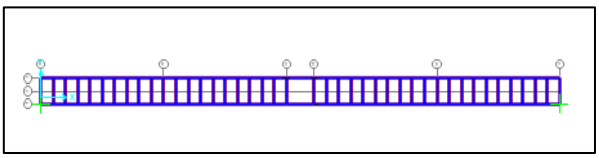

Fig.4: Plan view

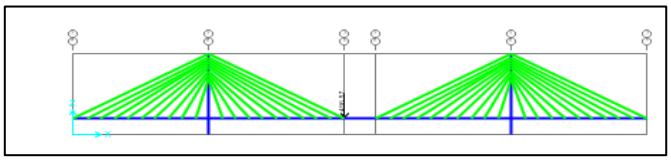

Fig. 5: Front view

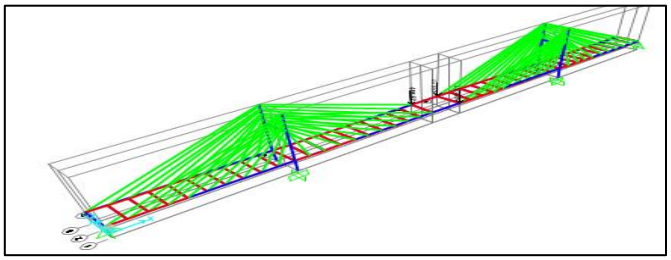

Fig. 6: 3D view

Above figure shows plan, front and 3D view of the cable stayed bridge in SAP 2000.

Power System Technology
ISSN:1000-3673
Received: 16-04-2025 Revised: 05-05-2025 Accepted: 22-06-2025

4. RESULTS

The results section presents a detailed analysis of the structural response of the cable-stayed bridge model under varying wind load conditions. The key parameters evaluated include displacement, base reaction, and bending moment, which are critical indicators of the bridge's performance. By simulating different wind angles and speeds across multiple climatic regions, the study provides insights into how these factors influence the overall stability and behavior of the bridge. Displacement results offer a view of the bridge's lateral and vertical movement under wind forces, while base reaction results highlight the forces exerted on the bridge supports. Additionally, the bending moment analysis reveals the internal stresses within the bridge components, crucial for understanding potential weak points and areas prone to failure. These findings are integral to assessing the structural resilience of the bridge and form the basis for the subsequent discussion and recommendations.

4.1 Maximum displacement in m

1. Pune region

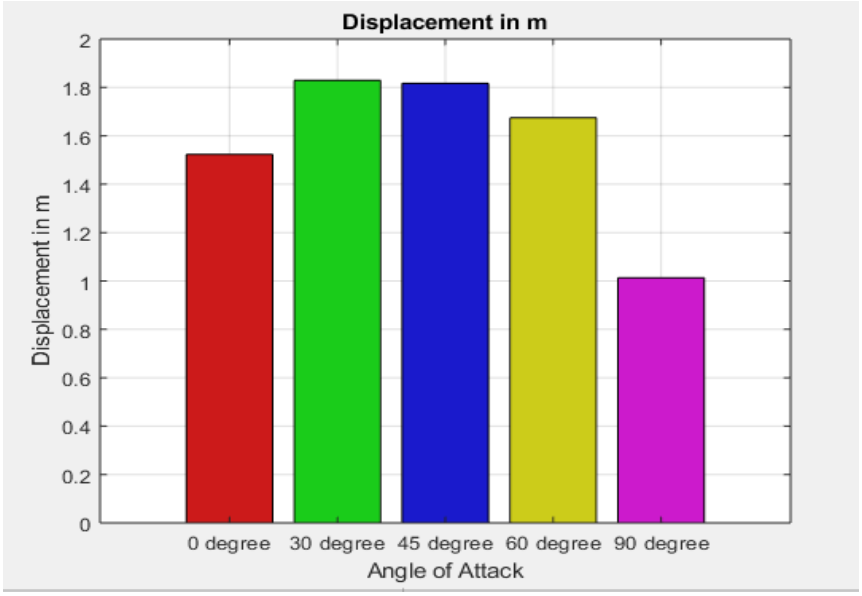

Graph 1: Maximum displacement in m for Pune region

The displacement response of the structure in the Pune area varies with angle of attack, with a peak at 30 degrees caused by higher lateral force components operating at this angle. As the angle increases to 45 and 60 degrees, the displacement decreases marginally, indicating a more stable response to larger angular stresses. The displacement is at its lowest point at 90 degrees, suggesting that the load operates more axially, resulting in less lateral displacement. This pattern illustrates how load direction affects structural behavior at varying attack angles.

Power System Technology
ISSN:1000-3673
Received: 16-04-2025 Revised: 05-05-2025 Accepted: 22-06-2025

2. Mumbai region

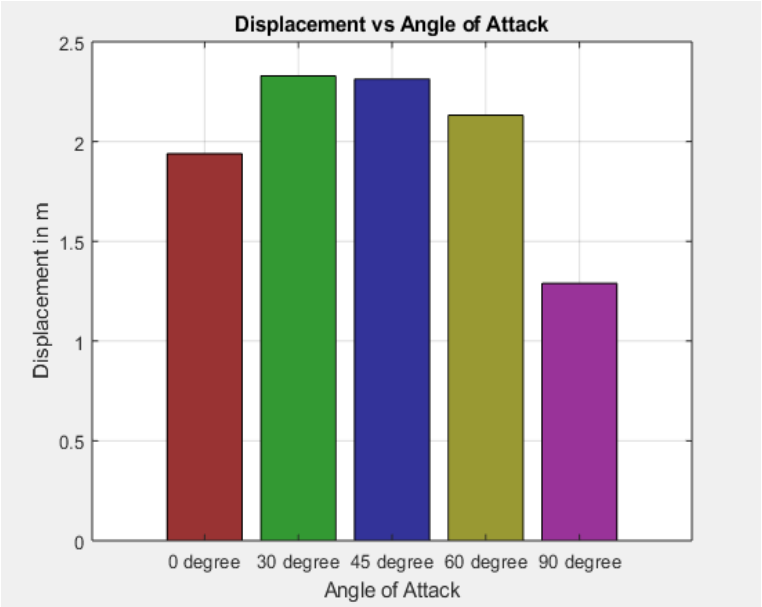

Graph 2: Maximum displacement in m for Mumbai region

In the Mumbai region, the displacement of the structure increases with the angle of attack, reaching a maximum at 30 degrees, likely due to the increased lateral load component. At 45 degrees, the displacement remains high but slightly decreases, indicating a minimal reduction in the lateral response. As the angle progresses to 60 degrees, the displacement drops, showing a stabilizing trend under larger angular forces. At 90 degrees, the displacement is at its lowest, suggesting that the load is primarily axial, minimizing lateral deformation. This behavior demonstrates the impact of load angle on the structural performance in the region.

3. Delhi region

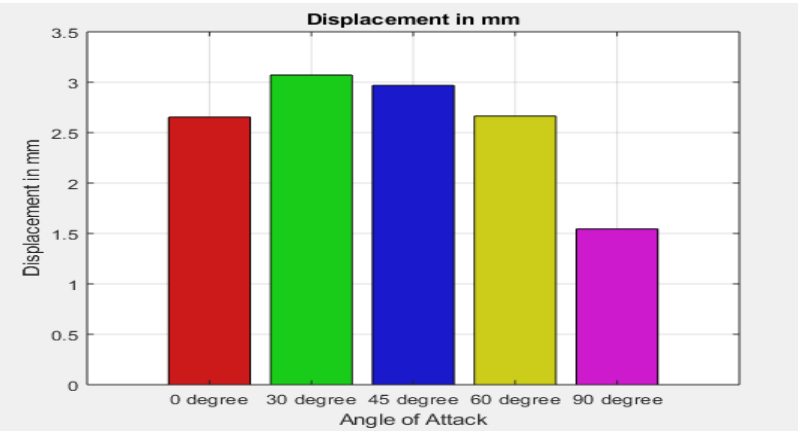

Graph 3: Maximum displacement in m for Delhi region

Power System Technology
ISSN:1000-3673
Received: 16-04-2025 Revised: 05-05-2025 Accepted: 22-06-2025

In the Delhi region, the structure exhibits maximum displacement at 30 degrees, where lateral forces are most pronounced. At 45 degrees, the displacement reduces slightly, indicating a marginal decline in the lateral impact. As the angle increases to 60 degrees, the displacement decreases m, showing a continued reduction in structural deformation. At 90 degrees, the displacement reaches its minimum value, suggesting that axial loading predominates, thereby minimizing lateral displacement. This trend highlights the varying influence of the angle of attack on the structure's lateral response.

4.2 Base reaction in KN

1. Pune region

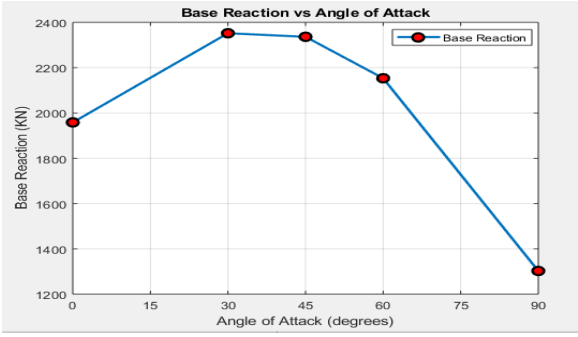

Graph 4: Base reaction in KN for Pune region

In the Pune region, the base reaction peaks at 30 degrees, indicating maximum lateral force impact at this angle. As the angle increases to 45 and 60 degrees, the base reaction decreases, with a significant drop at 90 degrees, suggesting that the load becomes more axial, reducing lateral force transmission.

2. Mumbai region

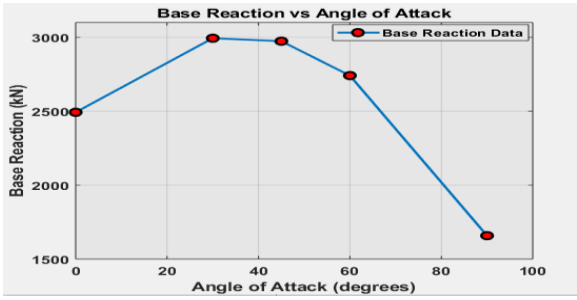

Graph 5: Base reaction in KN for Mumbai region

In the Mumbai region, the base reaction reaches its highest value at 30 degrees, reflecting the strongest lateral force effect. As the angle increases to 45 and 60 degrees, the base reaction gradually decreases, with a sharp reduction at 90 degrees, where the wind is perpendicular to the bridge, resulting in less force transferred to the supports due to a more distributed load across the side spans and pylons.

Power System Technology
ISSN:1000-3673
Received: 16-04-2025 Revised: 05-05-2025 Accepted: 22-06-2025

3. Delhi region

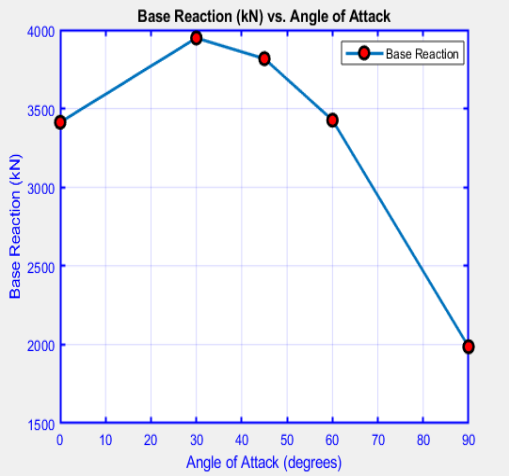

Graph 6: Base reaction in KN for Delhi region

In the Delhi region, the base reaction reaches its peak at 30 degrees, indicating the highest lateral force influence. As the angle increases to 45 and 60 degrees, the base reaction decreases progressively, with a significant drop at 90 degrees, suggesting a shift toward axial force dominance and reduced lateral load impact. These results highlight the critical impact of wind angle on base reactions, with the 30-degree angle presenting the most challenging condition for support forces in the Delhi region.

4.3 Bending moment in KNm

1. Pune region

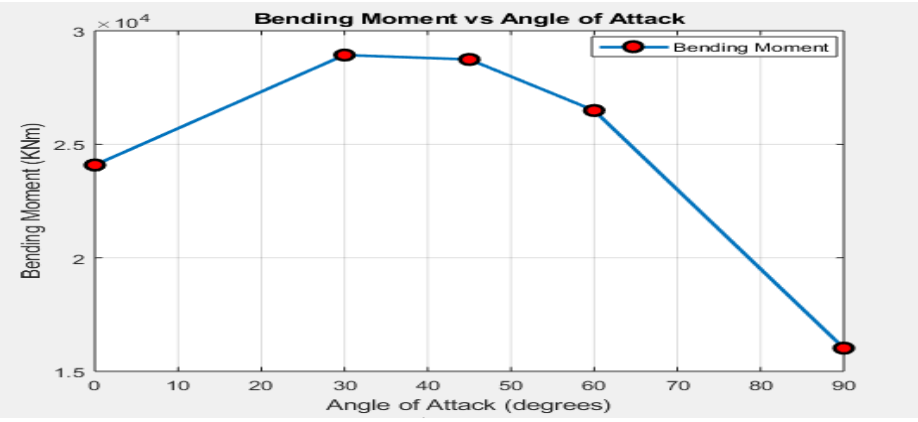

Graph 7: Bending moment in KNm for Pune region

Power System Technology
ISSN:1000-3673
Received: 16-04-2025 Revised: 05-05-2025 Accepted: 22-06-2025

The bending moment results for the Pune region illustrate how different angles of attack impact the internal stresses within the cable-stayed bridge. The bending moment reaches its maximum at 30 degrees, indicating the highest flexural demand due to lateral loading. As the angle increases to 45 and 60 degrees, the bending moment gradually reduces, with a significant decrease at 90 degrees, reflecting a predominantly axial load condition.

2. Mumbai region

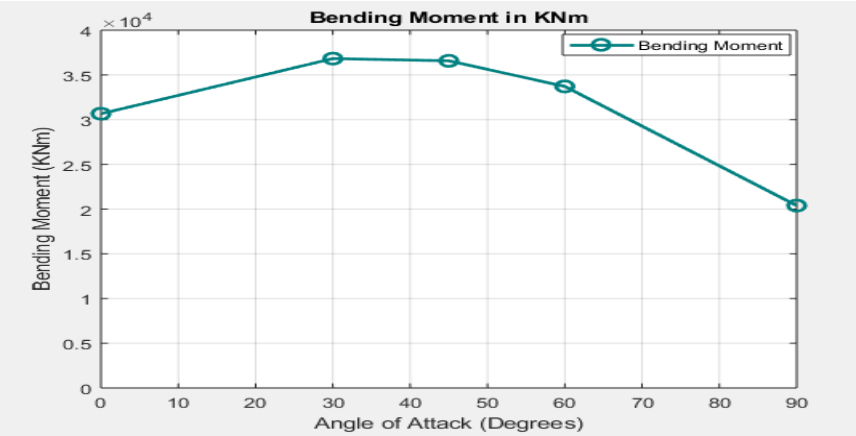

Graph 8: Bending moment in KNm for Mumbai region

In the Mumbai region, the bending moment peaks at 30 degrees, showing maximum flexural stress due to lateral forces. As the angle shifts to 45 and 60 degrees, the bending moment decreases, with a substantial drop at 90 degrees, indicating a transition toward axial load dominance, where the wind is perpendicular to the bridge, resulting in reduced internal stresses due to the wind load being more evenly distributed across the side spans and pylons.

3. Delhi region

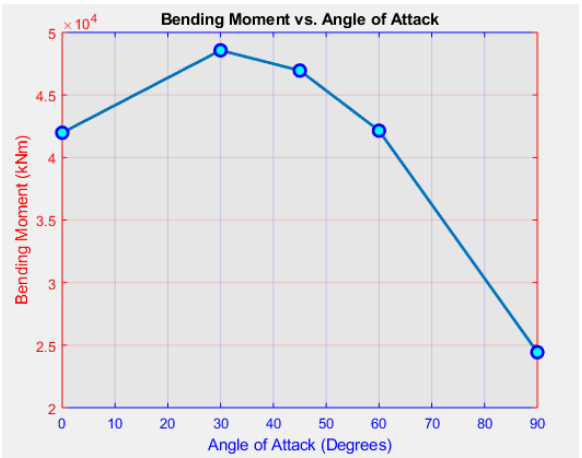

Graph 9: Bending moment in KNm for Delhi region

Power System Technology
ISSN:1000-3673
Received: 16-04-2025 Revised: 05-05-2025 Accepted: 22-06-2025

In the Delhi region, the bending moment is maximized at 30 degrees, indicating the highest flexural stress due to lateral loads. As the angle increases to 45 and 60 degrees, there is a slight reduction in the bending moment, followed by a significant decrease at 90 degrees, which suggests a shift towards axial load effects.

5. CONCLUSION

In conclusion, this research emphasizes the need of knowing wind load effects on cable-stayed bridges, which are becoming more common in contemporary infrastructure due to their aesthetic appeal and structural efficiency. The results show that the dynamic behavior of these bridges is very sensitive to variations in wind angles and speeds, demanding a detailed examination during the design process to reduce the dangers associated with aerodynamic instability. The use of sophisticated modeling tools, such as those found in SAP2000, is helpful in reproducing real-world circumstances and analyzing structural performance under a variety of environmental situations.

This research paper presents a complete parametric analysis of the effects of wind load on cable-stayed bridges, with an emphasis on the complex interactions between varying wind angles and climatic conditions. Using modern finite element analysis software, notably SAP2000, the research painstakingly evaluates the Quincy Bayview Bridge, emphasizing its unique structural characteristics such as double-plane stay cables and strong concrete pylons. In compliance with IS 875 (Part 3) requirements, the examination includes a broad variety of wind angles (0°, 30°, 45°, 60°, and 90°) and speeds that represent varied climatic settings such as Pune, Mumbai, and Delhi. The findings provide light on the bridge's dynamic behavior under various wind conditions, indicating major weaknesses linked to progressive collapse and overall structural integrity. By identifying important performance indicators, the research hopes to improve the design and optimization of cable-stayed bridges, ultimately contributing to the creation of more robust structures capable of withstanding dynamic environmental loads.

The research used a methodical approach, beginning with the development of a realistic model of the Quincy Bayview Bridge, which captured its complicated geometry and material qualities. The analysis provided substantial insights into the bridge's dynamic response to wind loads, with predictions indicating the possibility of collapse under certain situations. Wind load studies, accounting for wind speeds and angles, revealed that at a wind speed of 39 m/s (Pune), the computed wind loads varied dramatically across angles, with a maximum windward load of around 2632.56 kN at 30°. This pattern maintained with wind speeds of 44 m/s (Mumbai) and 47 m/s (Delhi), with significantly different loading dynamics, underscoring the relevance of wind direction in the structural response of cable-stayed bridges.

The following comparative conclusions and discussions are inferred:

- The angle of attack has a specific influence on bridge deflection in Pune, Mumbai, and Delhi regions. At 30 degrees, all regions show the highest displacements, with Delhi having the greatest deflection (3.071041 meters), followed by Mumbai (2.328372 meters) and Pune (1.829263 meters). This shows that the 30-degree angle causes the most substantial lateral displacement owing to the combined influence of longitudinal and transverse wind

Power System Technology
ISSN:1000-3673
Received: 16-04-2025 Revised: 05-05-2025 Accepted: 22-06-2025

forces at all locations. At 45 degrees, displacements reduce marginally compared to 30 degrees, with Delhi suffering the highest deflection (2.968762 meters), indicating persistent susceptibility to oblique wind conditions. The lowest displacements occur at 90 degrees, when the wind is perpendicular to the bridge. Pune has the least deflection (1.012983 meters), showing superior performance in terms of decreased lateral movement. The 30-degree angle regularly causes the highest displacement, notably in Delhi, making it the most important condition for deflection. In contrast, the 90-degree angle produces the least displacement across all regions, with Pune achieving the best results in terms of decreased deflection.

- A comparison investigation of base reactions in Pune, Mumbai, and Delhi shows how varying angles of attack affect the forces encountered by the bridge supports. At 30 degrees, the base reactions are strongest in all regions, with Delhi having the highest force (3948.846 kN), followed by Mumbai (2993.897 kN) and Pune (2352.126 kN). This implies that the 30-degree angle places the most stress on the supports owing to the combined impacts of longitudinal and transverse wind forces. At 45 degrees, the base reactions remain strong, with Delhi (3817.331 kN) still experiencing large forces, but significantly reduced in comparison to 30 degrees. The base reactions drop at 60 degrees, indicating a reduction in forces, with Pune (2153.433 kN) having the lowest reaction among the regions. The lowest base reactions are seen at 90 degrees, with Pune (1302.527 kN) receiving the least force, suggesting a more uniformly distributed load and improved performance in terms of reduced support forces. Overall, the 30-degree angle produces the highest base reactions, particularly in Delhi, making it the most crucial condition for support forces, while the 90-degree angle produces the best outcomes in terms of reduced base reactions, with Pune displaying the best performance.
- An examination of bending moments in Pune, Mumbai, and Delhi shows how different angles of attack impact internal stresses in cable-stayed bridge. At 30 degrees, all regions suffer the greatest bending moments, with Delhi recording the highest value (48570.8029 kNm), indicating that this angle causes the most severe internal stresses due to the combined effects of longitudinal and transverse wind forces. Mumbai follows with a bending moment of 36824.9286 kNm, while Pune has a somewhat lower moment of 28931.1551 kNm. At 45 degrees, the bending moments remain large, with Delhi exhibiting high internal stresses (46953.1755 kNm), but marginally reduced from 30 degrees. The moments fall at 60 degrees, with Delhi having a bending moment of 42147.7795 kNm, indicating a decrease in internal stresses as the wind direction changes. The lowest bending moments occur at 90 degrees, with Delhi (24431.3011 kNm) having the least internal stress, followed by Mumbai (20392.3828 kNm) and Pune (16021.0817). This implies that the wind perpendicular to the bridge produces the best conditions in terms of reduced internal stresses. Overall, the 30-degree angle causes the highest internal bending moments, particularly in Delhi, making it the most crucial condition for internal stresses, while the 90-degree angle produces the best outcomes in terms of reduced bending moments, with Pune demonstrating the best performance.

Power System Technology
ISSN:1000-3673
Received: 16-04-2025 Revised: 05-05-2025 Accepted: 22-06-2025

This research not only expands the information base about the performance of cable-stayed bridges, but it also gives practical insights for engineers and designers looking to improve bridge resilience. Overall, the results highlight the need of careful wind analysis in the design of cable-stayed bridges, which are prone to dynamic loads. The study provides significant insights into improving bridge designs for improved performance and safety, making it an essential resource for engineers and designers in the field. Future research may look at other environmental elements and structural configurations to increase the resilience and dependability of cable-stayed bridges in the face of various climatic difficulties.

REFERENCES

1. Fleming, J. F., & Egeseli, E. A. (1980). Dynamic behaviour of a cable-stayed bridge. Earthquake Engineering & Structural Dynamics, 8(1), 1–16. https://doi.org/10.1002/eqe.4290080102
2. Martins, A. M. B., Simões, L. M. C., & Negrão, J. H. J. O. (2020). Optimization of cable-stayed bridges: A literature survey. Advances in Engineering Software, 149, 102829. https://doi.org/10.1016/j.advengsoft.2020.102829
3. Maniar, O., Khanwilkar, P., & Sable, S. (2020). Effect of Wind on Cable Stayed Bridges.
4. Mendis, P., Ngo, T., Haritos, N., Hira, A., Samali, B., & Cheung, J. (2007). Wind loading on tall buildings. Electronic Journal of Structural Engineering, 1, 41–54. https://doi.org/10.56748/ejse.641
5. Zhu, X., Jiang, Y., & Weng, G. (2024). Study of the dynamic reaction mechanism of the cable-stayed tube bridge under earthquake action. Buildings, 14(7), 2209. https://doi.org/10.3390/buildings14072209
6. Eklund, G. (1972). General features of vibration-induced effects on balance. Upsala Journal of Medical Sciences, 77(2), 112–124. https://doi.org/10.1517/03009734000000016
7. Babu, R., & Prasad, R. (2018). Wind induced vibrations on cable stayed bridges, 4(1).
8. Javanmardi, A., Ghaedi, K., Huang, F., Hanif, M. U., & Tabrizikahou, A. (2022). Application of structural control systems for the cables of cable-stayed bridges: State-of-the-art and state-of-the-practice. Arch. Computational Methods in Engineering, 29(3), 1611–1641. https://doi.org/10.1007/s11831-021-09632-4
9. Svensson, H., & Svensson, H. (2012). Cable-stayed bridges: 40 years of experience worldwide (1st ed.). Berlin: Ernst, Wiley-Blackwell.
10. Walther, R. (1999). Cable Stayed Bridges. Emerald Publishing Limited. Retrieved from https://www.google.co.in/books/edition/Cable_Stayed_Bridges/AhSgrMcT4sgC?hl=en&gbpv=0
11. Martins, A. M. B., Simões, L. M. C., & Negrão, J. H. J. O. (2020). Optimization of cable-stayed bridges: A literature survey. Advances in Engineering Software, 149, 102829. https://doi.org/10.1016/j.advengsoft.2020.102829
12. Martins, A. M. B., Simões, L. M. C., & Negrão, J. H. J. O. (2020). Optimization of cable-stayed bridges: A literature survey. Advances in Engineering Software, 149, 102829. https://doi.org/10.1016/j.advengsoft.2020.102829
13. Chenari, H. M., Sheikhani Nejad, M. A. R., Agha, F. N. J., Jensi, Z., & Kahaki, F. (2021). Providing a model of agritourism in rural development: Case study: Masal County, Guilan

Power System Technology
ISSN:1000-3673
Received: 16-04-2025 Revised: 05-05-2025 Accepted: 22-06-2025

Province, Iran. Journal of Agricultural Science - Sri Lanka, 16(1), 93–107. https://doi.org/10.4038/jas.v16i1.9187
14. Kasuga, A., Arai, H., Breen, J. E., & Furukawa, K. (1995). Optimum cable-force adjustments in concrete cable-stayed bridges. Journal of Structural Engineering, 121(4), 685–694. https://doi.org/10.1061/(ASCE)0733-9445(1995)121:4(685)
15. Wang, J., et al. (2022). Influence of rapid curing methods on concrete microstructure and properties: A review. Case Studies in Construction Materials, 17, e01600. https://doi.org/10.1016/j.cscm.2022.e01600
16. Janjic, D., Pircher, M., & Pircher, H. (2003). Optimization of cable tensioning in cable-stayed bridges. Journal of Bridge Engineering, 8(3), 131–137. https://doi.org/10.1061/(ASCE)1084-0702(2003)8:3(131)
17. Chawla, R. N., Goyal, P., & Saxena, D. (2023). Exploring the drivers of digital transformation in Indian organizations: A multi-sector study. International Journal of Information Systems Change Management, 13(3), 234–264. https://doi.org/10.1504/IJISCM.2023.133362
18. Lee, T.-Y., Kim, Y.-H., & Kang, S.-W. (2008). Optimization of tensioning strategy for asymmetric cable-stayed bridge and its effect on construction process. Structural and Multidisciplinary Optimization, 35(6), 623–629. https://doi.org/10.1007/s00158-007-0172-9
19. Sung, Y.-C., Chang, D.-W., & Teo, E.-H. (2006). Optimum post-tensioning cable forces of Mau-Lo Hsi cable-stayed bridge. Engineering Structures, 28(10), 1407–1417. https://doi.org/10.1016/j.engstruct.2006.01.009
20. Sun, H., Dou, Y.-Z., & Qian, Y.-J. (2009). Optimal cable tension design for cable-stayed bridges on trust region algorithm. In International Conference on Transportation Engineering 2009 (pp. 1826–1831). American Society of Civil Engineers. https://doi.org/10.1061/41039(345)302
21. Baldomir, A., & Hernández, S. (2009). Cable optimization of a long span cable stayed bridge in La Coruña (Spain). In OPTI 2009 (pp. 107–119). Algarve, Portugal. https://doi.org/10.2495/OP090101
22. Baldomir, A., Hernandez, S., Nieto, F., & Jurado, J. A. (2010). Cable optimization of a long span cable stayed bridge in La Coruña (Spain). Advances in Engineering Software, 41(7–8), 931–938. https://doi.org/10.1016/j.advengsoft.2010.05.001
23. Hernandez, S., Baldomir, A., & Perez, I. (2012). Optimization of cable cross-sectional area in long span cable stayed bridges. In 20th Analysis and Computation Specialty Conference (pp. 278–287). Chicago, Illinois, United States. https://doi.org/10.1061/9780784412374.025
24. Zhang, T., & Bai, H. F. (2011). Analysis of cable-stayed bridge for APDL-based optimization. Advanced Materials Research, 243-249, 1567–1572. https://doi.org/10.4028/www.scientific.net/AMR.243-249.1567
25. Yu, B. C., Gao, S. X., Gao, C., Yang, J., & Xie, B. (2012). The determination of the problem of the cable-stayed bridge reasonable superpositioning optimization under the constant load state, based on the unknown load coefficient method of Midas/Civil. Applied Mechanics and Materials, 178–181, 2081–2084. https://doi.org/10.4028/www.scientific.net/AMM.178-181.2081

Power System Technology
ISSN:1000-3673
Received: 16-04-2025 Revised: 05-05-2025 Accepted: 22-06-2025

26. Hassan, M. M., Nassef, A. O., & El Damatty, A. A. (2012). Determination of optimum post-tensioning cable forces of cable-stayed bridges. Engineering Structures, 44, 248–259. https://doi.org/10.1016/j.engstruct.2012.06.009
27. Sun, S. J., Gao, J., & Huang, P. M. (2013). Forward-calculating optimization method for determining the rational construction state of cable-stayed bridges. Advanced Materials Research, 671–674, 980–984. https://doi.org/10.4028/www.scientific.net/AMR.671-674.980
28. Lonetti, P., & Pascuzzo, A. (2014). Design analysis of the optimum configuration of self-anchored cable-stayed suspension bridges. Structural Engineering and Mechanics, 51(5), 847–866. https://doi.org/10.12989/SEM.2014.51.5.847
29. Soutter, A. R. B., & Mõttus, R. (2020). 'Global warming' versus 'climate change': A replication on the association between political self-identification, question wording, and environmental beliefs. Journal of Environmental Psychology, 69, 101413. https://doi.org/10.1016/j.jenvp.2020.101413
30. Martins, A. M. B., Simões, L. M. C., & Negrão, J. H. J. O. (2015). Cable stretching force optimization of concrete cable-stayed bridges including construction stages and time-dependent effects. Structural and Multidisciplinary Optimization, 51(3), 757–772. https://doi.org/10.1007/s00158-014-1153-4
31. Asgari, B., Osman, S. A., & Adnan, A. B. (2015). Optimization of pre-tensioning cable forces in highly redundant cable-stayed bridges. International Journal of Structural Stability and Dynamics, 15(1), 1540005. https://doi.org/10.1142/S0219455415400052
32. Song, C., Xiao, R., & Sun, B. (2018). Optimization of cable pre-tension forces in long-span cable-stayed bridges considering the counterweight. Engineering Structures, 172, 919–928. https://doi.org/10.1016/j.engstruct.2018.06.061
33. Sung, Y.-C., Wang, C.-Y., & Teo, E.-H. (2016). Application of particle swarm optimization to construction planning for cable-stayed bridges by the cantilever erection method. Structural Infrastructural Engineering, 12(2), 208–222. https://doi.org/10.1080/15732479.2015.1008521
34. Carpentieri, G., Modano, M., Fabbrocino, F., Feo, L., & Fraternali, F. (2016). On the optimal design of cable-stayed bridges. In Proceedings of the VII European Congress on Computational Methods in Applied Sciences and Engineering (ECCOMAS Congress 2016) (pp. 3386–3394). Crete Island, Greece: Institute of Structural Analysis and Antiseismic Research School of Civil Engineering National Technical University of Athens. https://doi.org/10.7712/100016.2042.9574
35. Ha, M.-H., Vu, Q.-A., & Truong, V.-H. (2018). Optimum design of stay cables of steel cable-stayed bridges using nonlinear inelastic analysis and genetic algorithm. Structures, 16, 288–302. https://doi.org/10.1016/j.istruc.2018.10.007
36. Pacheco, P., & Magalhaes, F. (2015). Optimization of cable weight in multi-span cable-stayed bridges. In Multi-Span Large Bridges (pp. 511–518). CRC Press. https://doi.org/10.1201/b18567-62
37. García-Delgado, Y., et al. (2021). Prehabilitation for bariatric surgery: A randomized, controlled trial protocol and pilot study. Nutrients, 13(9), 2903. https://doi.org/10.3390/nu13092903

Power System Technology
ISSN:1000-3673
Received: 16-04-2025 Revised: 05-05-2025 Accepted: 22-06-2025

38. Arellano, H., Tolentino, D., & Gómez, R. (2019). Optimum criss-crossing cables in multi-span cable-stayed bridges using genetic algorithms. KSCE Journal of Civil Engineering, 23(2), 719–728. https://doi.org/10.1007/s12205-018-5736-2
39. Comartin, C. D., Niewiarowski, R. W., Freeman, S. A., & Turner, F. M. (2000). Seismic evaluation and retrofit of concrete buildings: A practical overview of the ATC 40 document. Earthquake Spectra, 16(1), 241–261. https://doi.org/10.1193/1.1586093
40. Pillai, S. U. (2012). Reinforced Concrete Technology. McGraw-Hill Education (India) Private Limited.
41. Krishna, M. M., C. D., & J-S. (2016). IS: 875(Part3): Wind Loads on Buildings and Structures - Proposed Draft & Commentary.